Journal of Fluids and Structures 18 (2003) 79–92

JOURNAL OF FLUIDS AND STRUCTURES

www.elsevier.nl/locate/jnlabr/yjfls

Flow excited resonance of a confined shallow cavity in low Mach number flow and its control

S. Ziada[a,*], H. Ng[b], C.E. Blake[a]

[a] *Department of Mechanical Engineering, McMaster University, Hamilton, Ont., Canada L8S 4L7*
[b] *AECL, Mississauga, Ont., Canada*

Received 3 July 2002; accepted 30 May 2003

Abstract

Shallow cavities exposed to unbounded, low Mach number flow are generally weak aeroacoustic sources because their acoustic modes are heavily damped. This paper focuses on a cavity mounted on the wall of a duct to investigate the effect of "confinement", i.e., solid boundaries close to the cavity, on the aeroacoustic response of shallow cavities in low Mach number flow ($M < 0.3$). It is found that the transverse acoustic modes of the duct–cavity combination are excited by the higher-order modes of the cavity shear layer oscillations. The nature of the excitation mechanism as well as the effects of the cavity and duct dimensions are investigated by means of measurements of the amplitude and phase distributions of the acoustic pressure, complemented with flow visualization of the cavity shear layer oscillation. A method to predict the onset of resonance is also suggested. It is also shown that the acoustic resonance is effectively suppressed by a feedback control method, which generates a synthetic jet acting at the cavity upstream corner. The effect of the phase and gain of the controller transfer function is studied in some detail.

1. Introduction

Flow-excited acoustic oscillations in cavities exposed to grazing flow have been the subject of extensive research since the early work by Krishnamurty (1955) and Roshko (1955). Several authors reviewed the state of knowledge for different flow regimes and cavity configurations (e.g., Rockwell and Naudascher, 1978; Rockwell, 1983; Komerath et al., 1987; Chokani, 1992). Rectangular cavities are generally classified as either *shallow or deep*, depending on whether the cavity length (L) is larger or smaller than its depth (D). In the former case, if the flow separating from the upstream corner reattaches to the downstream corner, the cavity is classified as *open shallow cavity*, but if the flow reattaches to the cavity floor, upstream of the downstream corner, the cavity is then *closed*. The present work deals with *open shallow cavities* mounted on the wall of a conduit, which conveys low Mach number flow.

Most investigations of shallow cavities, for which $L/D > 1$, consider moderate and high Mach number flows ($M > 0.4$); see for example, Rossiter (1964), Bilanin and Covert (1973), Heller and Bliss (1975) and many other papers as reviewed by Chokani (1992). This seems to have been driven by the fact that in many aeronautical applications, shallow cavities are often strong tone generators at high Mach number flows. Heller and Bliss (1975) attributed this tone generation to a coupling mechanism between the cavity shear layer oscillations and standing sound waves in the longitudinal direction inside the cavity. Although the details of the cavity geometry and the flow conditions are known to affect the cavity oscillations, the excitation mechanism, in general, consists of the following main events: (a) amplification of small disturbances in the shear layer; (b) generation of sound power due to convection of the unsteady

*Corresponding author. Tel.: +1-905-525-9140; fax: +1-905-572-7944.
E-mail address: ziadas@mcmaster.c (S. Ziada).

0889-9746/$ - see front matter © 2003 Elsevier Ltd. All rights reserved.
doi:10.1016/S0889-9746(03)00083-5

shear layer vorticity within the sound field; (c) enhancement of the resonant sound field by the sound power generated by the shear layer; and (d) the resonant sound field closes the feedback loop by generating new disturbances in the shear layer near its separation location.

Since the acoustic modes of shallow cavities are heavily damped due to sound radiation, as shown by Tam (1976), the excitation of these modes requires a high-energy level from the hear layer oscillation; a condition that could be satisfied only at relatively high Mach numbers. Although cavity oscillations can still occur at low Mach numbers (Rockwell, 1983), the oscillation amplitude in this case is generally small in comparison with those resulting from acoustic resonances of cavities at high Mach numbers.

Cavities may be surrounded by solid boundaries in close proximity in many practical applications, e.g., cavities in gas transport pipelines, steam piping systems, HVAC ducts, control valves, turbomachines and solid propellant motors. In these cases, acoustic reflections may reduce the radiation losses substantially and thereby increases the liability of the system to flow excited acoustic resonances. The object of this paper is to investigate the effect of confinement on the aeroacoustic response of shallow cavities exposed to low Mach number flows.

Another objective of the present work is to study the effect of feedback control on the excited acoustic resonance. It is worth noting that feedback control of impinging shear flow oscillations is not new and its effectiveness has been illustrated by several authors including Ziada (1995, 1999, 2000), Cattafesta et al. (1997) and Williams et al. (2000). In the present case, however, the resonant mode is predominantly a duct resonance mode excited by a higher-order mode of the shear layer oscillations. Additionally, a synthetic jet is used here to impart the control effect to the flow at the upstream edge of the cavity. This jet is directed at a 45° angle with the flow direction. The controllability of the duct resonance as a function of phase and amplitude of the synthetic jet oscillations is of primary importance in developing strategies, actuators and techniques to actively attenuate flow-induced noise.

2. Experimental setup

2.1. Test facility

The test facility consisted of three parts: an inlet section, a test-section and a diffuser section. The inlet section was a parabolic rectangular contraction, which insured uniform velocity profile within 2% at the inlet of the test-section. As shown in Fig. 1, the test-section was 559 mm in length and had a rectangular cross-section of height 254 mm and width of 76 mm. It was made of 25.4 mm thick, clear acrylic to facilitate flow visualization. All connections were sealed with O-rings in grooves to eliminate acoustic leakage from the test-section. The cavity was mounted on the top wall of the test-section, with its leading edge at 178 mm downstream of the test-section inlet. The cavity depth was kept constant at 50.8 mm, but the length was changed by adding a block at its downstream portion as illustrated by the shaded area in Fig. 1. The cavity lengths were $L = 127$ and 203.2 mm, which yielded length to depth ratios of $L/D = 2.5$ and 4.

A flat-walled diffuser that expands in one direction only, with an included angle of 14°, was used downstream of the test-section to increase the pressure recovery and thereby increase the maximum flow velocity during the tests. The diffuser outlet was connected to the inlet of a centrifugal blower equipped with a variable speed controller. The blower produced a maximum flow velocity of 105 m/s in the test-section, which facilitated tests up to a Mach number of $M \approx 0.3$.

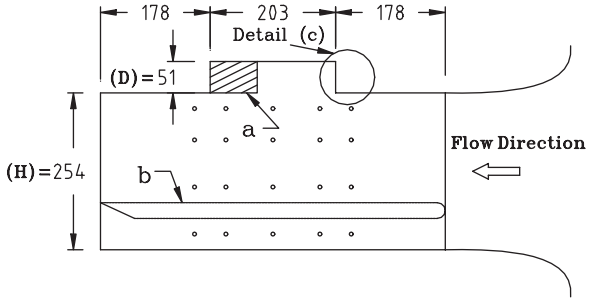

Fig. 1. Schematic of test-section showing inlet contraction, cavity, and splitter plate (b). The small circles show locations of pressure measurements, and the shaded area (a) represents a block, which is used to alter the cavity length. Details (c) of the upstream corner is shown in Fig. 2. Dimensions are in millimeter.

In order to change the height of the test-section H, or the height ratio H/D, a splitter plate was inserted in the test-section as shown in Fig. 1. To eliminate flow separation and possible vortex shedding excitations from the plate (Greenway and Wood, 1973; Stokes and Welsh, 1986), the leading edge was rounded and the trailing edge was beveled on one side to an included angle of 25°. This arrangement produced two different height ratios: $H/D = 3.5$ and 5, with and without the splitter plate, respectively. Additional details of the test setup can be found in Ng (2000).

Thus, four basic geometries were investigated: two cavity lengths $L/D = 2.5$ and 4, each of which was studied with two height ratios $H/D = 3.5$ and 5. In the rest of this paper, these cases will be referred to as Cases L and S, for the long and short cavities without the plate, and Cases LP and SP for the same cavities but with the plate.

2.2. Synthetic jet generator and controller

As shown in Fig. 2, the synthetic jet was generated by two, 50 W loudspeakers 100 mm in diameter. They were mounted behind the two sides of the cavity upstream corner. The cavity upstream corner was designed such that it accommodated a slit, at 45° with respect to the flow, that is connected to a small volume excited by the loudspeakers. The thickness of this slit could be adjusted by a slide mechanism that allowed the upstream wall of the cavity to move vertically (i.e., normal to the flow direction). The thickness of this slit was kept at 5 mm during the control tests. The gap between the speaker's cone and the facing wall was kept small, 12 mm, to increase the acoustic pulsation through the slit. As described by Smith and Glezer (1998), the speaker excitation generated a synthetic jet through the slit at 45° with the mean flow. This arrangement was used only when the effect of feedback control was being studied. During all other tests, this slit was completely closed by sliding the cavity upstream wall downwards, as shown in Fig. 2.

The controller used in this research was housed on a Pentium III personal computer and programmed in Simulink. It allowed the adjustment of gain and time delay of the controller output. The time delay adjustment produced a phase change in the controller output. The signal from a microphone sensing the pressure fluctuation inside the cavity was captured at a sampling rate of 20 kHz by a 12 bits A/D-D/A card (Quanser MQ3 DAQ) and used as input to the controller, whose output activated the speakers. The gain and delay settings for each test condition that achieved maximum attenuation of fluctuating force were located through a systematic search, e.g., by changing the delay time while keeping the gain constant. A more detailed description of the experimental apparatus and control system can be found in Ng (2000).

2.3. Instrumentation

As shown by the small circles in Fig. 1, an array of pressure taps was drilled on a sidewall as well as along the center-line of the cavity "floor", i.e., on the top wall of the test-section. Four $\frac{1}{4}$in condenser microphones were used simultaneously to measure the wall pressure fluctuations at different locations. Auto- and cross-power spectra together with phase data of the microphone signals were acquired by means of a 16-bit, four-channel data-acquisition board in conjunction with LabView software. In these measurements, the reference microphone was located inside the cavity at $x/L = 0.8$ and 0.875 for the short and long cavities, respectively, where x is measured from the cavity leading edge.

A pitot-static probe was used to measure the mean flow velocity, while the velocity fluctuation was acquired by means of a hotwire probe in conjunction with DISA anemometer.

The shear layer oscillation during acoustic resonance was visualized by injecting dense fog through a small hole drilled at the upstream edge of the cavity. A strobe light was used to slow the motion of the shear layer oscillation and the image was then recorded by means of a digital video camera.

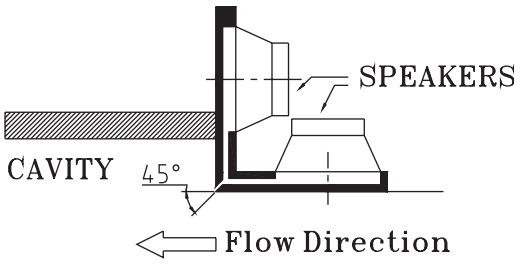

Fig. 2. Schematic of the cavity upstream corner, the loudspeakers and the exit slit of the synthetic jet.

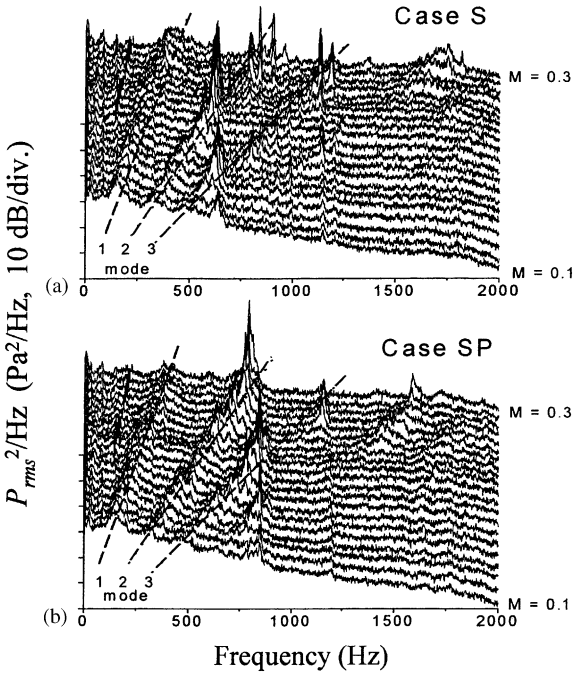

Fig. 3. Development of power spectral densities of pressure fluctuation inside the cavity with Mach number M. Short cavity: $L/D = 2.5$; (a) Case S: without splitter plate; and (b) Case SP: with splitter plate.

3. Overview of acoustic response

The development of pressure fluctuations inside the cavity for Cases S and SP is illustrated in Fig. 3 as a function of the Mach number, $M = U/C$, where U is the flow velocity and C is the speed of sound. The figure shows typical waterfall plots of power spectra of pressure fluctuations measured on the cavity floor at a distance of $0.8L$ from the leading edge. Each spectrum is the average of 50 data samples. The waterfall plots span a Mach number range of 0.1–0.3, with an increment of 0.01.

In each plot of Fig. 3, at least three spectral peaks can be seen whose frequencies increase approximately linearly with the Mach number. These peaks, which are indicated by the broken lines and referred to as modes 1, 2 and 3, are generated by the oscillation of the cavity shear layer at its lowest three modes $m = 1$, 2 and 3, where m refers to the number of vortices that can be formed in the shear layer. As will be shown later, the order of these modes (i.e., $m = 1$, 2 or 3) has been identified from comparisons of the measured Strouhal number with those reported in the literature and also from flow visualization of the shear layer oscillations. The lowest, or the fundamental mode, $m = 1$, is the strongest as can be seen in the spectra corresponding to nonresonant conditions, e.g., at low Mach numbers. It should be noted that the peaks of the *shear layer modes* are relatively broad banded, which indicates that these oscillations are rather weak and incoherent.

In Case S, Fig. 3(a), an acoustic resonance mode near 620 Hz is seen to be excited, first, by the third shear layer mode, $m = 3$ near $M = 0.15$, and then by the second mode, $m = 2$ near $M = 0.22$. Similar features can be seen in Case SP with the splitter plate, Fig. 3(b), except that the plate increases the frequency of the resonance mode from about 620 to 800 Hz.

4. Effect of cavity and duct dimensions

The frequency and the dimensionless amplitude ($P_{\text{r.m.s.}}/1/2\rho U^2$) of the dominant peaks in pressure spectra, taken from Fig. 3, are plotted as functions of Mach number in Figs. 4 and 5, for Cases S and SP, respectively. In both cases, the frequencies of the shear layer modes follow a constant Strouhal number relationship. The frequencies of these modes, at a given Mach number, are similar in both cases because the cavity length is the same. However, the resonance frequencies are higher in Fig. 5, which is caused by the presence of the plate. In the case without the plate, Fig. 4 shows

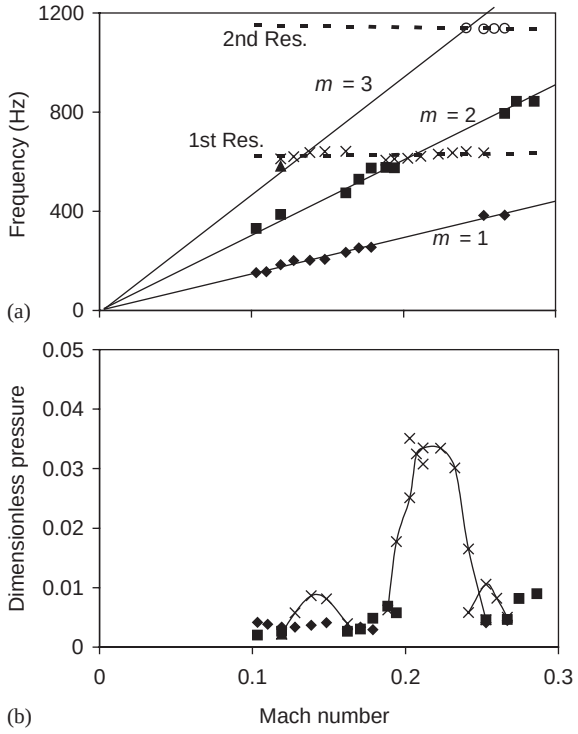

Fig. 4. Frequency and dimensionless amplitude of pressure fluctuation inside the cavity as functions of Mach number. Short cavity; $L/D = 2.5$; *without* splitter plate. Shear layer modes: ♦, $m = 1$; ■, 2; ▲, 3; ×, first resonance mode; ○, second resonance mode.

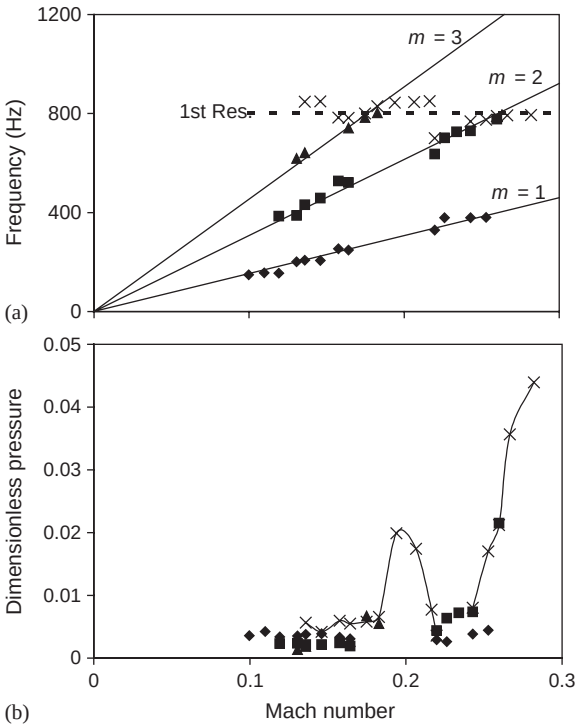

Fig. 5. Frequency and dimensionless amplitude of pressure fluctuation inside the cavity as functions of Mach number. Short cavity; $L/D = 2.5$; *with* splitter plate. Shear layer modes: ♦, $m = 1$; ■, 2; ▲, 3; ×, first resonance mode.

Table 1
Observed Strouhal numbers, S_m, of shear layer modes for the tested four cases in comparison with those reported by Heller and Bliss (1975)

Mode (m)	Case				Heller and Bliss (1975)[a]
	S	SP	L	LP	
1	0.54	0.56	0.45	0.44	—[b]
2	1.12	1.13	1.09	1.09	1.06–1.15
3	1.7	1.67	1.68	1.68	1.56–1.65

[a] For $L/D = 2-3.3$ and $M = 0.2$.
[b] Strouhal number for $m = 1$ was not observed.

that the lowest resonance mode is first excited, albeit weakly, by the third mode of the shear layer ($m = 3$) and then by the second mode ($m = 2$). At higher Mach numbers, $M = 0.25$, the second resonance mode is excited by the third mode of the shear layer. Similar features can be seen in Fig. 5, for the case with the plate, except that the resonances occur at higher Mach numbers because their frequencies are higher. For example, resonance of the second mode in Case SP could not be reached within the tested range of Mach number.

Scrutiny of Figs. 4 and 5 shows that the resonance of a particular acoustic mode is stronger when it is excited by a lower mode of the shear layer. Moreover, the oscillation amplitudes of the shear layer modes are relatively small compared with those observed during the resonance range. An additional feature is the slight, but discernible, increase in the resonance frequency within the resonance range. This frequency increase is an inherent feature of cavity resonance, Graf and Ziada (1992), because the effect of the cavity shear layer oscillation changes from an added mass to a stiffness effect as the flow velocity is increased.

Similar tests were conducted for the long cavity with and without the splitter plate. The results were found to be similar for the cases discussed above and therefore are not given here. As expected, at a given Mach number, the frequencies of the shear layer modes were lower than those in the short cavity case and therefore acoustic resonances in the long cavity cases occurred at higher Mach numbers.

The Strouhal numbers of the cavity shear layer modes are given in Table 1 for the tested four cases. The Strouhal number is defined as

$$S_m = \frac{f_m L}{U}, \tag{1}$$

where f_m is the frequency of shear layer mode m and U the flow velocity. The observed values for $m = 2$ and 3 agree well with those reported by Heller and Bliss (1975) for a Mach number of 0.2. Heller and Bliss did not observe oscillation at $m = 1$ up to a Mach number of 0.5. Tam and Block (1978) also observed oscillations at the higher-order modes, but not at the fundamental $m = 1$. For the present confined cavity, the duct walls reflect the sound generated by the shear layer oscillations, and this reflection seems to promote the shear layer oscillations at the *fundamental mode* at substantially lower Mach numbers than in the case of unconfined cavities.

As can be seen in Table 1, the Strouhal number decreases slightly as the ratio L/D increases. Similar trends were reported by Heller and Bliss (1975) and Ethembabaoglu (1973) for $L/D > 2$.

5. Acoustic and shear layer modes

In this section, the nature of the resonant acoustic mode as well as the source of excitation are confirmed by means of correlation measurements and flow visualization. During the initial set of experiments, it was anticipated that the resonance frequency would be related to the cavity length as reported in the literature, e.g., by Rockwell and Naudascher (1978). However, the results showed that the resonance frequency did not scale with the cavity length. As can be seen from Table 2, changing the cavity length from 127 to 203 mm, corresponding to Cases S and L, respectively, did not alter the resonance frequency. The splitter plate was therefore used to explore the effect of the duct height on the resonance frequency. For acoustic standing waves along the duct height, two length scales are of relevance: the duct height, H, and the total height at the cavity, $H + D$. The frequencies of the standing waves of the duct–cavity combination are expected to be within the frequency range estimated from these length scales. As shown in Table 2, the measured frequencies are within the estimated frequency range based on these heights.

Table 2
Comparison between the measured resonance frequencies and those predicted based on the length scales H and $H + D$

Test case	Range of predicted frequencies (Hz)	Measured frequency (Hz)
S	566–679	630
L	566–679	625
SP	755–970	795
LP	755–970	785

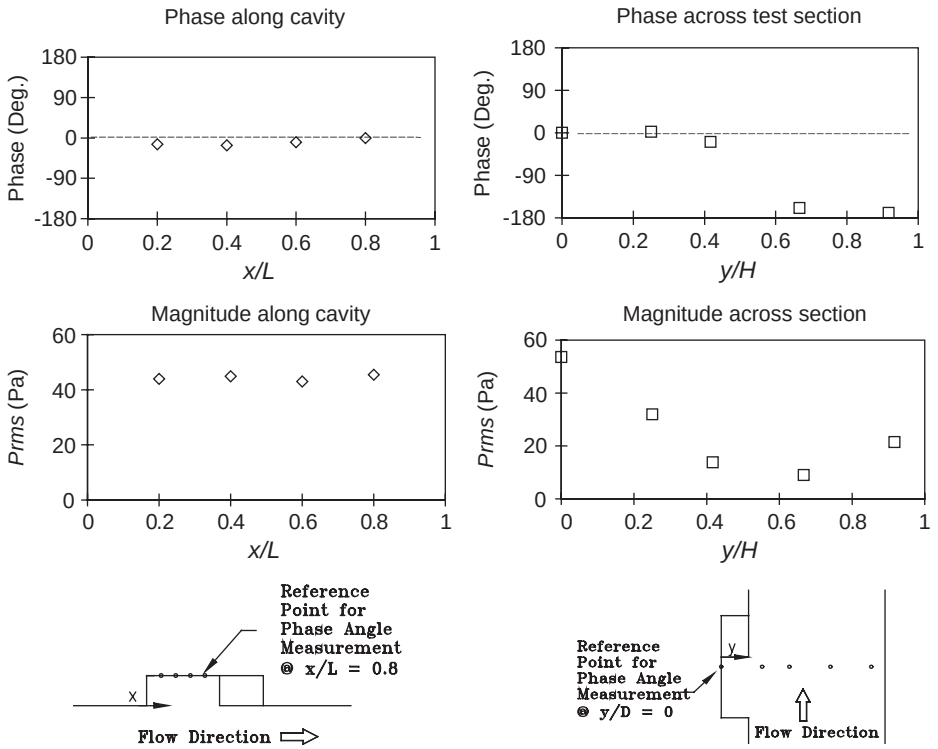

Fig. 6. Phase and amplitude distributions of the resonant acoustic mode for $L/D = 2.5$ and without the splitter plate. $M = 0.203$; left-hand side: distributions along the cavity floor; right-hand side: distributions across the duct.

The shape of the acoustic mode was also confirmed by measuring the amplitude and phase distributions of the pressure oscillation whilst the acoustic resonance was excited. Typical results are shown in Fig. 6 for Case S. The left-hand side of this figure shows that the acoustic pressure amplitude and phase are virtually constant along the cavity "floor". Thus, no longitudinal acoustic waves within the cavity are excited. The right-hand side of Fig. 6 shows clearly a standing wave pattern in the transverse direction, i.e., along the test-section height. These measurements were repeated for the other three cases and they all showed similar characteristics confirming that the excited mode consists of a one-half wavelength standing wave along the duct height at the location of the cavity.

As can be seen from Fig. 6, the cavity shear layer is located near a pressure maximum, where the acoustic particle velocity is rather small. This arrangement may suggest a weak interaction between the shear layer oscillation and the acoustic mode. Blevins (1985), for example, investigated the excitation of acoustic modes of a duct by vortex shedding from a cylinder in cross-flow. He showed that the resonance becomes weaker as the cylinder is moved away from center of the duct, which is the location of the maximum particle velocity of the acoustic mode. Since the shear layer in the present experiments is near the position of maximum acoustic pressure, a flow visualization study was conducted to confirm the shear layer coupling with the resonant sound field as well as its oscillation pattern (or mode m) at different resonant conditions.

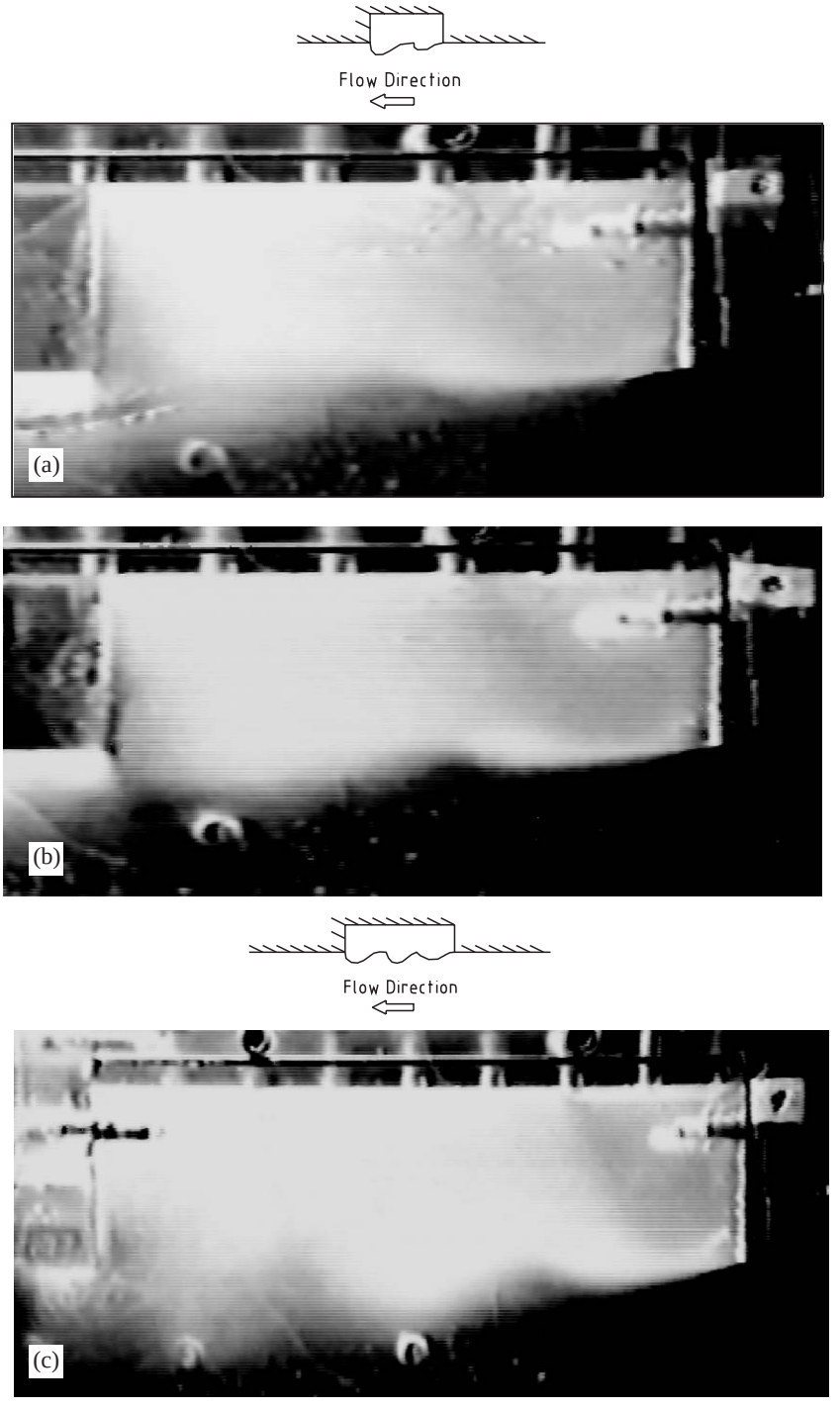

Fig. 7. Flow visualization photographs of the shear layer oscillation pattern whilst the first resonance mode is excited. (a) $L/D = 2.5$, $M = 0.203$, without splitter plate; (b) $L/D = 2.5$, $M = 0.282$, with splitter plate; and (c) $L/D = 4$, $M = 0.28$, with splitter plate.

Typical flow visualization photographs are shown in Fig. 7. The top two photographs correspond to acoustic resonance excitation by the second shear layer mode ($m = 2$), and therefore the shear layer oscillation shows two instability wavelengths. The bottom photograph corresponds to resonance excitation by the third shear layer mode

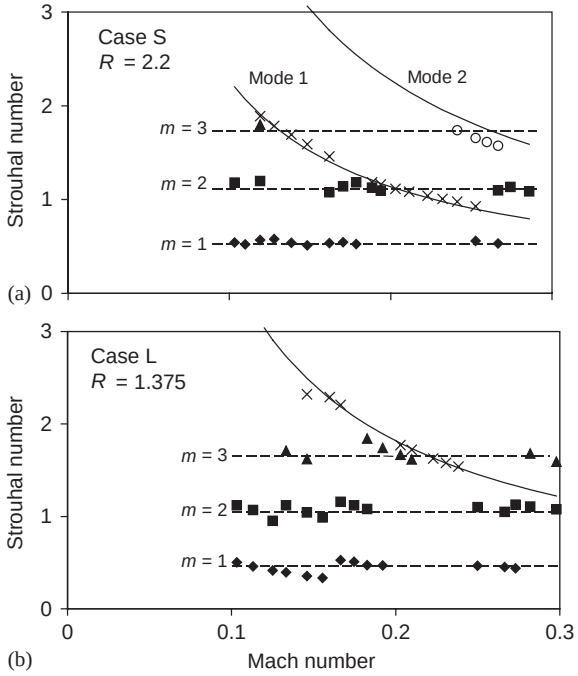

Fig. 8. Strouhal number versus Mach number plots of the dominant frequency components of pressure fluctuation inside the cavity. (a) Short cavity, $L/D = 2.5$, *without* splitter plate and (b) long cavity, $L/D = 4$, *without* splitter plate. Shear layer modes: ♦, $m = 1$; ■, 2; ▲, 3; ×, first resonance mode; ○, second resonance mode.

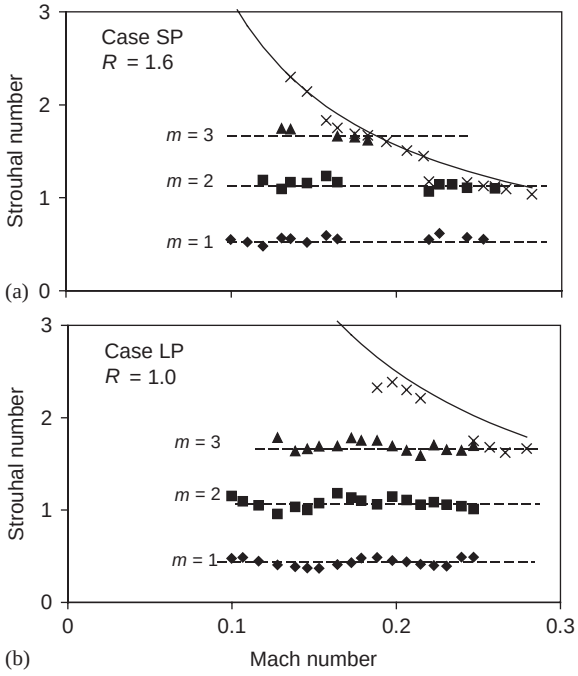

Fig. 9. Strouhal number versus Mach number plots of the dominant frequency components of pressure fluctuation inside the cavity. (a) Short cavity, $L/D = 2.5$, *with* splitter plate and (b) long cavity, $L/D = 4$, *with* splitter plate. Shear layer modes: ♦, $m = 1$; ■, 2; ▲, 3; ×, first resonance mode.

($m = 3$). The shear layer oscillation depicts three instability wavelengths along the mouth of the cavity. Thus, the higher-order modes of the shear layer oscillations ($m = 2$ and 3) seem to be strong sources of excitation in the present flow geometry despite the close proximity of the shear layer to the location of maximum acoustic pressure.

6. Prediction of resonance

The Strouhal number based on the resonance frequency, f_R, the cavity length, L, and the flow velocity, U, is given by

$$S_R = \frac{f_R L}{U}. \tag{2}$$

Since the resonance is found to occur in the transverse direction, the mean height of the duct–cavity combination, H_m, can be used to estimate the wavelength of the acoustic standing wave. It is clear that such an approach will yield only an approximate estimate of the resonance frequency:

$$f_R = \frac{kC}{2H_m} \quad \text{for } k = 1, 2, \ldots, \tag{3}$$

where C is speed of sound, H_m is given by

$$H_m = H + \frac{D}{2}. \tag{4}$$

Substituting Eq. (3) into Eq. (2) yields

$$S_R = \frac{k}{2RM}, \tag{5}$$

where M is the Mach number and $R = H_m/L$ is the *confinement ratio*, which is the ratio between the mean height of the duct and the cavity length. Figs. 8 and 9 show the Strouhal number versus the Mach number for all tested cases. In these figures, the solid curves represent Eq. (5), whereas the broken lines correspond to the Strouhal numbers of the shear layer modes. The confinement ratio is also given for each case.

Despite the crude approximation made in predicting the resonance frequency from the duct mean height, Eq. (5) is seen to give excellent predictions of the occurrence of acoustic resonance in a duct housing a shallow cavity exposed to low Mach number flow. This good correlation with the confinement ratio R is due to the fact that it relates the two relevant length scales; the first, H_m, determines the resonance frequency of the duct acoustic mode, and the second, L, dictates the frequency of the shear layer oscillation.

7. Feedback control of resonance

As mentioned earlier, several authors investigated the effect of open-loop and feedback control on shallow cavity resonance. For example, Cattafesta et al. (1997) were able to suppress cavity resonance by means of piezoelectric actuators, which were implemented at the cavity upstream corner. The synthetic jet approach used in the present work offers another means of control, which may be simpler and more efficient in some applications, especially at high frequencies. The object of this section is to study the effectiveness of this approach in suppressing acoustic resonances in shallow cavities when: (a) the resonance is excited by higher-order modes of the shear layer instability, and (b) when the synthetic jet is inclined to the main flow.

7.1. Control strategy

As shown in Fig. 10, Ziada (1995) formulated a strategy to suppress acoustic resonances excited by impinging shear flows. The crucial event of the excitation mechanism is the *feedback* from acoustic resonance, which induces new disturbances in the shear layer at the upstream corner of the cavity. As shown in Fig. 10, the objective is to use the synthetic jet to neutralize the feedback event of the excitation mechanism by counteracting the effect of the resonant acoustic mode at the upstream corner of the cavity.

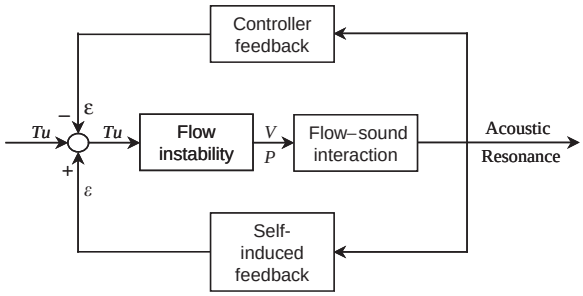

Fig. 10. Schematic presentation of the acoustic resonance mechanism together with the effect of the controller which is used to counteract the self-induced feedback, ε, at the upstream cavity corner. *Tu* stands for flow turbulence; V and P for velocity and pressure fluctuations (Ziada 1995).

7.2. System response with and without control

The effect of feedback control was studied for Case S, i.e., for the short cavity without the splitter plate. The Mach number during the control tests was kept constant at 0.22. At this Mach number, Fig. 4 shows that the first acoustic mode at 630 Hz was excited by the second mode of the shear layer instability.

As mentioned in the experimental setup, the signal of a microphone mounted inside the cavity was phase shifted, amplified and then fed to the speakers. The phase shift was introduced by imposing a time delay before activating the speakers. In order to investigate systematically the effect of this time delay, it was varied in steps of $\frac{1}{8}$ of the oscillation period T. The effect of the gain was also investigated in some detail. Selected spectra of pressure amplitude are given in Fig. 11 to illustrate the effect of control on the frequency content of cavity oscillations.

Fig. 11(a) corresponds to a time delay of $\frac{7}{8}T$ and a normalized gain of unity (the choice of unity gain is made only to illustrate the effect of increasing the gain by a given factor). It is seen that the spectral peak at resonance is almost eliminated without increasing the level of the broadband noise in the cavity. Increasing the normalized gain to 2, Fig. 11(b), results in a further decrease in the resonance peak, but other frequency components start to appear and become stronger with further increases in gain. For Fig. 11(c), the normalized gain is set at unity but the time delay is changed to $\frac{3}{8}T$ so that the speaker signal is 180° out of phase with that corresponding to Fig. 11(a). As expected, the controller enhances the resonance, but not as much as it reduces the resonance in case (a). For example, in Fig. 11(a), a reduction of 15 dB was achieved compared to an enhancement of only 2 dB in Fig. 11(c).

7.3. Effect of controller gain and time delay

The effect of normalized gain and time delay of the speaker signal is illustrated in Fig. 12. The time delay is given in terms of the oscillation period, T, and the control effect is quantified by the ratio between the maximum spectral peaks with and without control defined by

$$\text{Amplitude ratio} = 20\log\left(\frac{\text{maximum amplitude with control}}{\text{maximum amplitude without control}}\right)\text{(dB)}.$$

The time delay, or the phase, of the speaker signal is clearly the dominant parameter dictating the system response. Its effect is cyclic with a period similar to the period of cavity oscillation.

At a normalized gain of unity, the resonance intensity could be reduced, to varying degrees, over a wide range of time delay. The maximum amount of attenuation (≈ -15 dB) was much higher than the maximum amount of enhancement ($\approx +2$ dB). When the gain was doubled, the range of time delay for effective suppression became narrower, but the maximum reduction in the oscillation amplitude increased substantially. A time delay of $\frac{7}{8}T$ is considered optimum because it achieves the maximum attenuation. Moreover, at this value, the amount of attenuation is not so sensitive to small variations from the optimum time delay.

At a normalized gain of 3, the effect of control on the cavity oscillation continues to be cyclic. At the optimum time delay for the smaller gain cases, $\frac{7}{8}T$, the amount of attenuation decreased. This trend continued with increasing gain, but as long as the time delay was kept at the optimum value, $\frac{7}{8}T$, the oscillation amplitude was always smaller than that without control, although the normalized gain was increased up to a value of 10. This latter feature is illustrated in Fig. 13, which shows the effect of increasing the normalized gain from 1 to 10, while holding the time delay at its optimum value of $\frac{7}{8}T$.

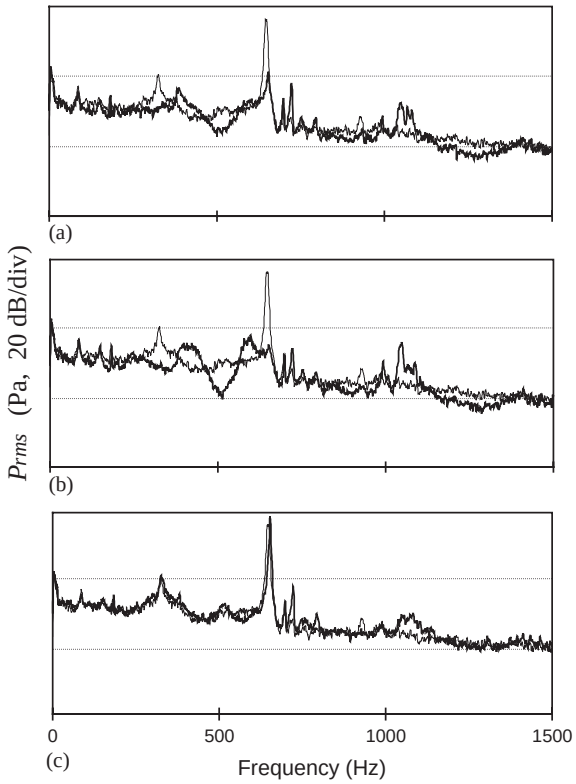

Fig. 11. Typical spectra of pressure fluctuations inside the cavity: thin line, without control; thick line, with control. (a) Gain = 1, delay = $\frac{7}{8}T$; (b) gain = 2, delay = $\frac{7}{8}T$; and (c) gain = 1, delay = $\frac{3}{8}T$.

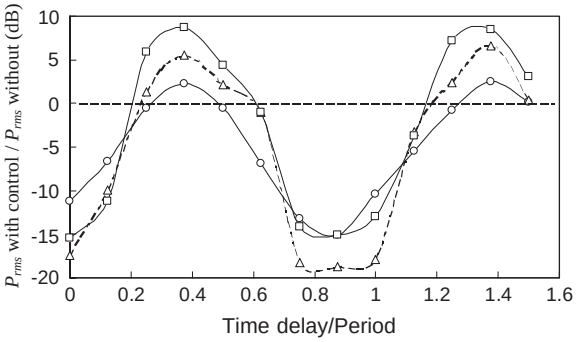

Fig. 12. Effect of the controller time delay and gain on the amplitude of pressure oscillations inside the cavity. ○, gain = 1; △, gain = 2; □, gain = 3.

Thus, the present results illustrate clearly the effectiveness of the developed simple control technique in eliminating the acoustic resonance of the duct.

8. Conclusions

Shallow cavities in flow ducts can generate powerful acoustic resonances at low Mach number flows. In contrast with the acoustic modes excited at high Mach numbers, which consist of longitudinal standing waves inside the cavity, those excited in the present study are transverse standing waves of the duct–cavity combination. The resonance is excited by

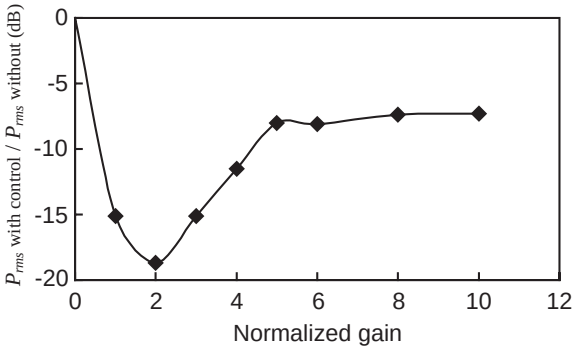

Fig. 13. Effect of controller gain on the amplitude of pressure oscillations inside the cavity. Time delay is set at $\frac{7}{8}T$ for all gains.

the higher-order modes of the shear layer oscillations ($m = 2$ and 3) and is stronger when it is excited by a lower shear layer mode. The onset of resonance can be estimated from the confinement ratio, which relates the duct height to the cavity length. Aside from the occurrence of resonance, the cavity confinement in the present experiments seems to promote the fundamental mode of the natural shear layer oscillations at substantially lower Mach numbers than in the case of unconfined cavities.

The acoustic resonance is excited by a coupling mechanism between the shear layer and the resonant field, which perpetrates the inducement of new disturbance in the shear layer. Counteracting the effect of this coupling by means of the synthetic jet suppresses the excitation mechanism and thereby eliminates the resonance. Although the shear layer is positioned near the location of *minimum* particle velocity of the resonant field, the interaction mechanism seems to generate enough acoustic energy to sustain the resonance.

The effect of the phase of the control signal is found to be cyclic such that the resonance is suppressed and enhanced in a cyclic manner as the phase angle (or the delay time) is increased. At the optimum setting of the phase angle, the amount of attenuation is less sensitive to small variations in the phase angle. This feature indicates that sufficient attenuation can be achieved even when the phase angle deviates slightly from the optimum setting.

Increasing the gain, at the optimum phase setting, reduces the resonance intensity gradually until the resonant oscillation is practically eliminated. Further increases in gain restore the oscillation, albeit at a frequency that is slightly lower than that without control. However, the oscillation amplitude attained with the maximum available gain, but at the optimum time delay, was still smaller than that occurred without control.

References

Bilanin, A.J., Covert, E.E., 1973. Estimation of possible excitation frequencies for shallow rectangular cavities. AIAA Journal 11, 347–351.

Blevins, R.D., 1985. The effect of sound on vortex shedding from cylinders. Journal of Fluid mechanics 161, 217–237.

Cattafesta III, L.N., Garg, S., Choudhari, M., Li, F., 1997. Active control of flow-induced cavity resonance. AIAA Paper No. 97-1804, AIAA, Washington, DC.

Chokani, N., 1992. Flow induced oscillations in cavities—a critical survey. AIAA Paper No. 92-02-159, AIAA, Washington, DC.

Ethembabaoglu, S., 1973. On the Fluctuating Flow Characteristics in the Vicinity of Gate Slots. Division of Hydraulic Engineering, Norwegian Institute of Technology, University of Trondheim (Quoted by Rockwell and Naudascher, 1978).

Graf, H.R., Ziada, S., 1992. Flow induced acoustic resonance of closed side branches: an experimental determination of the excitation source. Proceedings of the Third International Symposium on Flow-Induced Vibration and Noise, Vol. 7, ASME, New York, pp. 63–80.

Greenway, M.E., Wood, C.J., 1973. The effect of bevelled trailing edge on vortex shedding and vibration. Journal of Fluid Mechanics 61, 323–335.

Heller, S.S., Bliss, D.B., 1975. The physical mechanism of flow induced pressure fluctuations in cavities and concepts for their suppression. AIAA Paper No. 75-491, AIAA, Washington, DC.

Komerath, N.M., Ahuja, K.K., Chambers, F.W., 1987. Prediction and measurement of flows over cavities—a survey. AIAA Paper No. 87-0166, AIAA, Washington, DC.

Krishnamurty, K., 1955. Acoustic radiation from two-dimensional rectangular cutouts in aerodynamic surfaces. NACA Technical Note No. 3487, NACA, USA.

Ng, H., 2000. Acoustic resonance of confined shallow cavities in low Mach number flow. Master's Thesis, Mechanical Engineering, McMaster University, Hamilton, Ontario, Canada.

Rockwell, D., 1983. Oscillations of impinging shear layers. AIAA Journal 21, 645–664.

Rockwell, D., Naudascher, E., 1978. Review—self-sustaining oscillations of flow past cavities. ASME Journal of Fluids Engineering 100, 152–165.

Roshko, A., 1955. Some measurements of flow in a rectangular cutout. NACA Technical Note No. 3488, NACA, USA.

Rossiter, J.E., 1964. Wind tunnel experiments of the flow over rectangular cavities at subsonic and transonic speeds. Aeronautical Research Council Reports and Memoranda No. 3438 UK.

Smith, B.L., Glezer, A., 1998. The formation and evolution of synthetic jets. Physics of Fluids 10, 2281–2297.

Stokes, A.N., Welsh, M.C., 1986. Flow–resonant sound interaction in a duct containing a plate, Part II: square leading edge. Journal of Sound and Vibration 104, 55–73.

Tam, C.K.W., 1976. The acoustic modes of a two-dimensional rectangular cavity. Journal of Sound and Vibration 49, 353–364.

Tam, C.K.W., Block, P.J.W., 1978. On the tones and pressure oscillations induced by flow over rectangular cavities. Journal of Fluid Mechanics 89, 373–399.

Williams, D.R., Fabris, D., Morrow, J., 2000. Experiments on controlling multiple acoustic modes in cavities. AIAA Paper No. 2000–1903, AIAA, Washington, DC.

Ziada, S., 1995. Feedback control of globally unstable flows: impinging flows. Journal of Fluids and Structures 9, 907–923.

Ziada, S., 1999. Feedback control of flow-excited cavity resonance. In: M.J. Pettigrew (Ed). Flow-Induced Vibration 1999, ASME Publication No. 389, ASME, New York, pp. 325–330 (Also in Journal of Fluids and Structures 15, 831–843).

Ziada, S., 2000. Active stabilisation of a planar jet impinging on a flexible wedge. In: S. Ziada, T. Stanbli (Eds). Proceedings of Seventh International Conference on Flow-Induced Vibration, Lucerne, Switzerland, Balkema, Amsterdam, pp. 187–194 (Also in Journal of Fluids and Structures 16, 613–626).